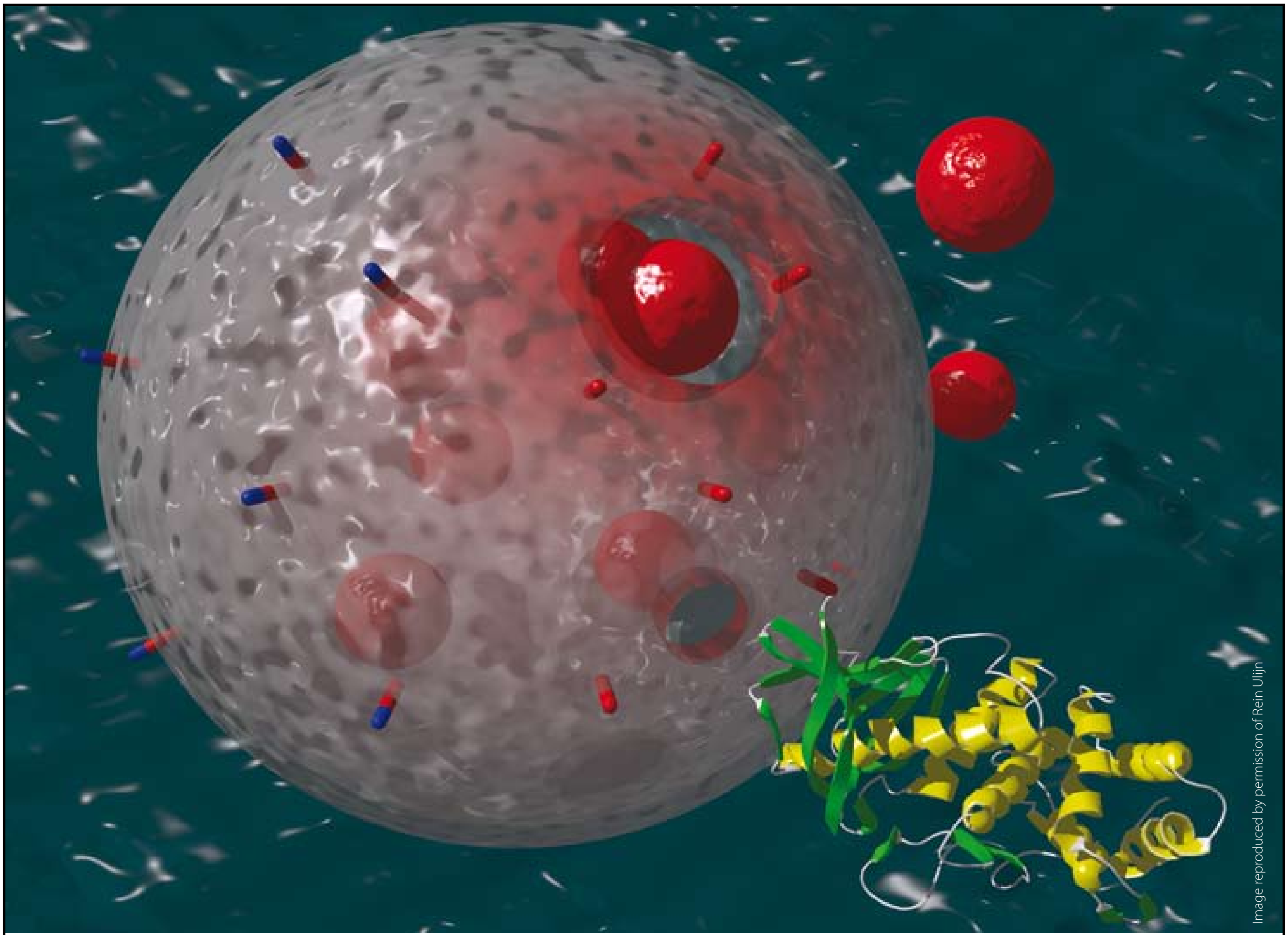

Image reproduced by permission of Rein Ulijn

Showcasing research from the Ulijn and Webb labs, University of Manchester

Title: Enzyme-responsive hydrogel particles for the controlled release of proteins: designing peptide actuators to match payload

This work describes polymer hydrogel particles that release a protein payload when triggered by selective action of protease enzymes through peptide-based actuators. Peptide actuator design rules are described that allow for tunable protein release profiles based on (mis)-matching of charge distributions to those on the released protein.

As featured in:

Paul D. Thornton, Robert J. Mart, Simon J. Webb and Rein V. Ulijn, *Soft Matter*, 2008, **4**, 821

23080793

Enzyme-responsive hydrogel particles for the controlled release of proteins: designing peptide actuators to match payload†

Paul D. Thornton,[a] Robert J. Mart,[b] Simon J. Webb[b] and Rein V. Ulijn*[a]

Received 25th September 2007, Accepted 9th January 2008
First published as an Advance Article on the web 8th February 2008
DOI: 10.1039/b714750c

We report on enzyme-responsive hydrogel particles for the controlled release of proteins. Amino-functionalised poly(ethylene glycol acrylamide) (PEGA) hydrogel particles were functionalised with peptide actuators that cause charge-induced swelling and payload release when triggered enzymatically. Peptide-based actuators were designed to match the specificity of the target enzyme, while also matching the charge properties of the to-be released protein payload, thereby uniquely allowing for tuneable release profiles. Fluorescently labelled albumin and avidin, proteins of similar size but opposite charge, were released at a rate that was governed by the peptide actuator linked to the polymer carrier, offering a highly controlled release mechanism. Release profiles were analysed using a combination of fluorescence spectroscopy of the solution and two-photon fluorescence microscopy to analyse enzymatically triggered molecular events within hydrogel particles during the initial stages of release.

1. Introduction

Materials to which one or more properties can be altered through the application of an external stimulus are described as being responsive. Such materials can sense their environment and respond to it in a manner that may be exploited in applications such as biosensing, tissue regeneration and controlled release.[1] The response may be governed by inherent material properties or may be a consequence of chemical or biochemical functionalisation. Numerous systems have been devised that respond to external stimuli such as temperature, ionic strength, solvent polarity, electric/magnetic fields, light or small (bio-)molecules.[1]

In addition to the stimuli listed above, an intensive focus has recently been placed on the use of enzymes to trigger a macroscopic response. Enzymes offer key advantages as release triggers; they are not biologically disruptive, function under mild conditions, and possess a high degree of selectivity. Enzyme-responsive materials are therefore increasingly investigated in the context of applications in drug delivery, as they offer spatiotemporal control of drug release by particular enzymes, or combinations of enzymes, which are (over-)expressed in affected regions in most disease states.[2]

We recently introduced PEG-based hydrogel particles functionalised with charged peptide actuators to control the enzyme-triggered release of macromolecules under constant pH, temperature and ionic strength. In this system, enzyme-compatible[3] poly(ethylene glycol acrylamide), ($PEGA_{800}$)[4] particles were functionalised with zwitterionic peptides composed of enzyme-cleavable peptides flanked by oppositely charged amino acids (Fig. 1A). Upon exposure to the target enzyme (thermolysin), selective enzymatic hydrolysis of the enzyme-cleavable peptide resulted in the release of anionic fragments, leaving anchored cationic fragments that convert the neutral PEGA particles into cationic particles. This charge switch resulted in particle swelling and a significant increase in overall particle diameter, a visual indication of increased internal mesh size.[5] This method allowed the triggered release of entrapped proteins that had been pre-loaded into the particles. However, preliminary results indicated that the release of negatively-charged macromolecules was poor, suggesting that electrostatic attraction between the host polymer and payload macromolecule was playing an important role. Herein we establish design rules for peptide actuators that will match the properties of the to-be released payload.

Avidin and albumin were chosen as model protein payload macromolecules because of their similar sizes (63 kDa and 66 kDa, respectively), opposite charges at physiological pH (avidin pI = 10.0, albumin pI = 4.7) and biological relevance. Indeed, there has been recent interest in serum proteins as carrier proteins for drug delivery.[6] Albumin–drug conjugates have been employed as prodrugs where the carrier protein both solubilises the drug and selectively releases the drug molecules at the intended site of action through an enzyme-cleavable peptide.[7]

The efficiency of two PEGA–peptide conjugates (Fig 1A,C) at releasing these macromolecules was compared. The first conjugate was zwitterionic Fmoc–Asp–Ala∼Ala–Arg–[PEGA] (**1**) which, following hydrolysis at the amide bond between alanine residues, left a H–Ala–Arg–[PEGA] sequence possessing two positive charges at physiological pH; on the Arg side chain and the terminal amine. We had demonstrated previously that this peptide–hydrogel conjugate could be used to successfully release cationic avidin,[5a] but preliminary results suggested that anionic albumin was retained and not released. We hypothesised that this behaviour was related to attractive interactions between

---

[a] *Manchester Interdisciplinary Biocentre (MIB) and School of Materials, University of Manchester, 131 Princess Street, Manchester, M1 7DN, UK. E-mail: rein.ulijn@manchester.ac.uk; Fax: +44 (0)161 306 8877; Tel: +44 (0)161 306 5986*
[b] *Manchester Interdisciplinary Biocentre (MIB) and School of Chemistry, University of Manchester, 131 Princess Street, Manchester, M1 7DN, UK*

† Electronic supplementary information (ESI) available: MALDI mass spectrometric data and relative pixel intensity plots. See DOI: 10.1039/b714750c

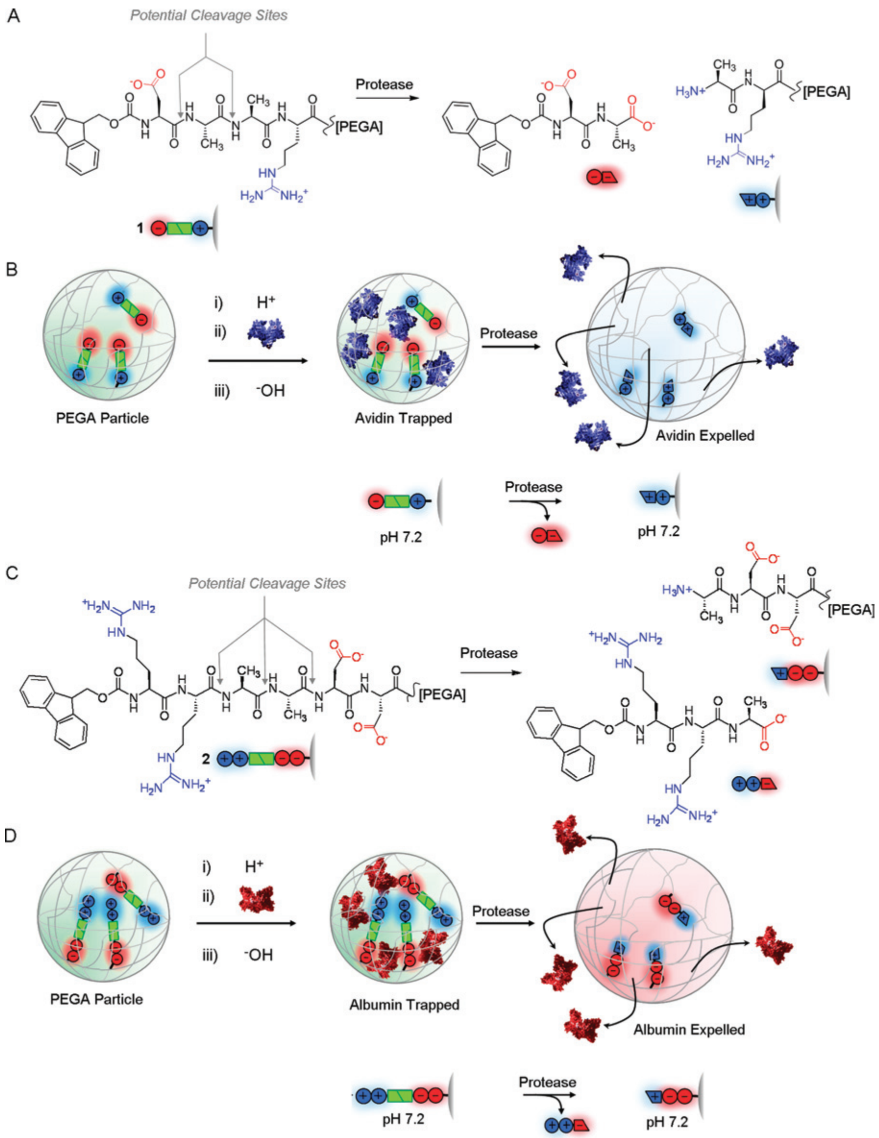

Fig. 1 A) The peptide designed for the release of positively charged proteins was comprised of Fmoc–aspartatic acid–alanine–alanine–arginine, where the amide bond between the two alanine residues is particularly liable to cleavage by our target enzyme. B) Generation of positive charges by enzymatic cleavage of the bond between alanine residues allows protein molecules to diffuse through the polymer pores for payload release. C) Peptide designed for the release of negatively charged protein molecules. Two N-terminal arginine units are separated from two aspartic acid groups by two alanine residues. A single net negative charge remains on the particle following enzymatic hydrolysis. D) Exclusion of albumin from the negatively charged swollen particle occurs following hydrolysis of the bond between alanine residues.

opposite charges within PEGA particles and payload protein. Thus, a second peptide sequence was designed that would produce negatively charged particles upon enzymatic hydrolysis, Fmoc–Arg–Arg–Ala∼Ala–Asp–Asp–[PEGA] (**2**); this design should allow the release of anionic proteins. Upon enzymatic hydrolysis an Ala–Asp–Asp–[PEGA] fragment is created that bears two negative charges on the aspartic acid side chains and a positive charge on the terminal amine, giving rise to a net single negative charge per sequence. Thus, the overall effect of enzymatic hydrolysis at physiological pH is a conversion from neutral to cationic particles for peptide actuator **1**, and neutral to anionic for **2** (Fig. 1D). Release profiles of the fluorescently labelled proteins were then analysed using a combination of fluorescence spectroscopy of the surrounding liquid phase and two-photon fluorescence microscopy to reveal molecular events within enzyme-triggered hydrogel particles when triggered enzymatically.

2. Experimental

2.1 Materials

Amino-functionalised PEGA$_{800}$ particles were supplied by VersaMatrix A/S (Denmark). Polymer hydrogel particles from a single batch (#105008, size range 150–300 μm) were used in all experiments. All other reagents and enzymes were supplied by Sigma-Aldrich unless otherwise stated. Fluorenylmethoxycarbonyl (Fmoc)-protected alanine, aspartic acid with a *tert*-butyl ester (O*t*Bu) side chain protecting group, and glycine were purchased from Bachem, protected arginine with a pentamethyldihydrobenzofuran-5-sulfonyl (Pbf) side chain protecting group was acquired from AGTC Bioproducts. Elastase was purchased from Worthington Chemical Company. HPLC water was supplied by Merck. Fisher Finest 75 mm × 25 mm glass slides and 22 mm × 22 mm cover slips were used for all microscopy techniques and were supplied by Fisher Scientific. Peptide coupling was performed in 3 mL Isolute SPE filtration columns, with removal of supernatants under vacuum by a Vacmaster 10 (both purchased from Kinesis).

2.2 Peptide coupling

Peptide chains were synthesised directly onto PEGA particles using stepwise Fmoc solid-phase peptide synthesis. Prior to initial chemical modification, the PEGA hydrogel particles were washed extensively with ethanol, methanol, and dimethylformamide (DMF). This washing procedure was also carried out between each coupling step. Di-isopropylcarbodiimide (DIC) and hydroxybenzotrioazole (HOBt) were used as the coupling agent and activating agent/racemisation inhibitor, respectively. HOBt (6 equivalents), DIC (6 equivalents), and the appropriately protected amino acid (3 equivalents) were dissolved in DMF (2 mL) and left to pre-activate for 10 minutes. The solution was then added to washed $\mathrm{PEGA_{800}}$ particles (100 mg) and placed on a blood rotor for 3 hours. The particles were then washed as described, and the coupling reaction repeated to ensure that complete coupling to all available amine sites was achieved ('double coupling'). Prior to the next amino acid coupling reaction, washing was repeated and the Fmoc group removed by reacting the particles with 20% piperidine in DMF solution for 2 hours. Removal of amino acid side-chain protecting groups was achieved by incubating the peptide-modified particles with 5% v/v water in trifluoroacetic acid (TFA) for two hours.

2.3 Protein loading – fluorescence spectroscopy

A Perkin Elmer LS 55 fluorescence spectrometer was used to compare the extent to which both Texas Red (TR)- and fluorescein isothiocyanate (FITC)-labelled proteins were loaded into peptide-modified particles. The respective protein solutions (1 mL, 1 mg $\mathrm{mL^{-1}}$) were diluted with distilled water (6.9 mL) and hydrochloric acid (0.1 mL, 0.1 M). Fluorescence spectra of these solutions were recorded (FITC excitation: 490 nm; emission: 520 nm. TR excitation: 520 nm; emission 583 nm), then the solutions (2 mL) were added to the appropriate peptide-modifed particles (50 mg) and agitated for two hours. The supernatants were filtered from the particles and the fluoresence spectra once more recorded. The integrated peak areas of emission spectra were calculated both before and after incubation with particles; the difference gave the amount of protein that had been loaded into the beads.

2.4 Enzymatic hydrolysis

The appropriate enzyme (2 mg $\mathrm{mL^{-1}}$ of lyophilised powder, or less as indicated) was dissolved in pH 7.4 phosphate buffer solution (0.01 M, 2 mL) and added to the peptide-functionalised $\mathrm{PEGA_{800}}$ beads (100 mg). Reactions were incubated overnight at room temperature before the supernatant solution was collected. An acetonitrile–water mixture (50% v/v, 8 mL) was used to wash the particles and ensure that all cleaved product had been removed from the hydrogel interior.

2.5 Particle swelling

Changes in particle swelling were observed using an Olympus IX 70 inverted microscope using standard Kohler illumination. A 40× objective was used to observe images of the particles on glass slides. Images were captured using a black and white charge-coupled device (CCD) camera (PixelFly, Cooke Corporation). Particles were suspended in the appropriate solution on a glass slide and covered with a glass cover slip. Images were obtained at minute intervals during the experiment. Image analysis was performed using Image J software; increases in particle diameter were readily determined as a function of increased pixel intensity.

2.6 Protein release – fluorescence spectrophotometry

A Perkin Elmer LS 55 fluorescence spectrophotometer was used to compare the extent of release of both TR- and FITC-labelled proteins from peptide-modified particles. Peptide-modified particles (50 mg) were incubated with 2 mL of enzyme solution. The reaction was stopped at the appropriate time point by removing the supernatant from the filtration column by vacuum filtration. The particles were rinsed with water (1 mL) which was added, along with the supernatant, to a 3 mL fluorescence cuvette. Integrated peak areas of emission spectra were calculated to quantify release of labeled proteins.

2.7 Protein release – two-photon microscopy

Microscopic analysis of the release experiments was carried out using a two-photon microscope with a Ti–Sapphire laser (Mira, Coherent) tuned to a wavelength of 770 nm, emitting pulses of 249 fs duration. This was coupled into a scanhead (Bio-Rad 1024ES) connected to an inverted microscope (Nikon TE300). A 20×/0.75 numerical aperture air-immersion lens was used to focus the laser source into the sample. The emitted light from the sample was filtered using a 525/550 nm filter for FITC experiments, and 575/625 nm filter for TR experiments. Following peptide coupling the particles were washed with (each 3 times) DMF, 1 : 1 methanol–DMF, ethanol, methanol, and 0.01 M phosphate buffer solution. The particles were stored in buffer solution (0.01 M). The particles were washed with water and added to the enzyme solution. Images were taken each minute for the duration of the experiment and changes in pixel intensity to signify protein release were quantified using Image J.

2.8 Quantification of peptide cleavage

High performance liquid chromatography (HPLC) was employed to quantify the extent of peptide cleavage following enzyme hydrolysis. The system consisted of a Dionex P680 HPLC pump connected to a Macherey-Nagel C18 column of length 250 mm, internal diameter 4.6 mm and particle size 5 μm. A 20 μL sample aliquot was injected into the column at a flow rate of 1 mL min^{-1}. The gradient used was constant at 40% acetonitrile in water for 2.5 minutes gradually rising to 90% acetonitrile in water at 17.5 minutes. This concentration was kept constant until 20.5 minutes when the gradient was gradually decreased to 40% acetonitrile in water at 23.5 minutes. Peak retention times and peak areas were compared with known standards. The cleaved product was quantified by monitoring Fmoc absorbance at 310 nm.

3. Results and discussion

We first studied the ability of the target enzyme, thermolysin, to selectively hydrolyse conjugates **1** and **2**. Modified hydrogel particles **1** and **2** were incubated overnight with thermolysin, which has previously been demonstrated to cleave dialanine peptides[5a] and chymotrypsin, a control enzyme. As expected, incubation with chymotrypsin caused minimal cleavage of **1** (8%) or **2** (7%) as measured by HPLC. The small amount of cleaved peptide is most likely due to trypsin impurities in the chymotrypsin causing cleavage adjacent to Arg residues, which has been observed previously.[8] In contrast, incubation with thermolysin caused complete cleavage of both peptides (>99%).

Differential interference contrast (DIC) microscopy was employed to determine changes in swelling of the two PEGA conjugates, **1** and **2**, and a third type of peptide actuator, Fmoc–Asp–Gly~Gly–Arg–[PEGA] (**3**), following enzyme hydrolysis. DIC microscopy allows for discrete changes in transparent samples to be observed without the need for staining. Changes in particle diameter were recorded over time allowing the change in particle volume following enzyme hydrolysis to be calculated (Table 1). A good correlation between changes in particle volume and the extent of enzyme hydrolysis (by HPLC) was found for the three peptides tested. It was also observed that greater changes in volume occurred for **1** compared to **2** following comparable degrees of hydrolysis by thermolysin due to the extra charge generated on these peptides following hydrolysis.

Table 1 Changes in particle volume and quantification of cleaved peptide (as percentage of total loading, by HPLC) following enzymatic hydrolysis of three different peptide actuators

Peptide	Enzyme [a]	Δ Volume [b]	% Cleavage [c]
DAAR (**1**)	None	1.00	<0.1
DAAR (**1**)	Chymotrypsin	1.04	7.7
DAAR (**1**)	Elastase	1.50	>99
DAAR (**1**)	Thermolysin	1.66	>99
RRAADD (**2**)	None	1.00	<0.1
RRAADD (**2**)	Chymotrypsin	1.02	6.8
RRAADD (**2**)	Elastase	1.10	37
RRAADD (**2**)	Thermolysin	1.16	>99
DGGR (**3**)	None	1.00	<0.1
DGGR (**3**)	Chymotrypsin	1.00	1.5
DGGR (**3**)	Elastase	1.05	37
DGGR (**3**)	Thermolysin	1.10	53

[a] Chymotrypsin preferentially cleaves substrates with larger, hydrophobic groups in the P1 position (carbonyl end of amide bond), thermolysin prefers hydrophobic groups in the P1′ (amine end of the amide bond). Elastase prefers smaller, hydrophobic groups in both the P1 and P1′ positions.[9] [b] After 45 min. [c] After 12 h.

Next, we studied the enzyme-triggered release of proteins. Hydrogel particles were loaded with the appropriate protein payload by altering the environmental pH to swell the peptide-modified particles (Fig. 1B). We have previously demonstrated that in solutions with pH < 5, **1** exist in a swollen, cationic, form[5a] due to protonation of the Asp side chain carboxylate groups, which leaves the positive charge of the Arg residues. Particle swelling allows rapid protein diffusion into the particle core and loading of the particle interior with protein molecules. Replacement of the acidic solution with buffer at pH 7 entraps the protein within the collapsed, neutral, particle. The extent of protein loading within the particles was analysed by fluorescence spectroscopy, and the loading values of **1** and **2** are given in Fig. 2A. These data demonstrate that similar protein loadings can be achieved, regardless of the charges present on either the protein or the hydrogel bound peptides.

Fluorescence spectroscopy was then used to compare the release of TR-labelled albumin from **1** and **2** following incubation with both chymotrypsin and thermolysin (Fig 2B). As expected, albumin release was significantly greater following exposure of **1** to thermolysin compared to the control chymotrypsin. Peptide design influenced the extent of albumin release, **2** released three times more albumin compared to **1** over the same 180 minute time period. Having demonstrated controlled release of a negative protein, the release profile of fluorescein isothiocyanate (FITC)-labelled cationic avidin was studied. Gratifyingly, avidin showed the opposite release profile to albumin (Fig. 2C), with greater release from **1** compared to **2**, demonstrating that payload charge will dictate both the rate and quantity released from particles carrying different peptides. This offers a mechanism for the release of negatively charged

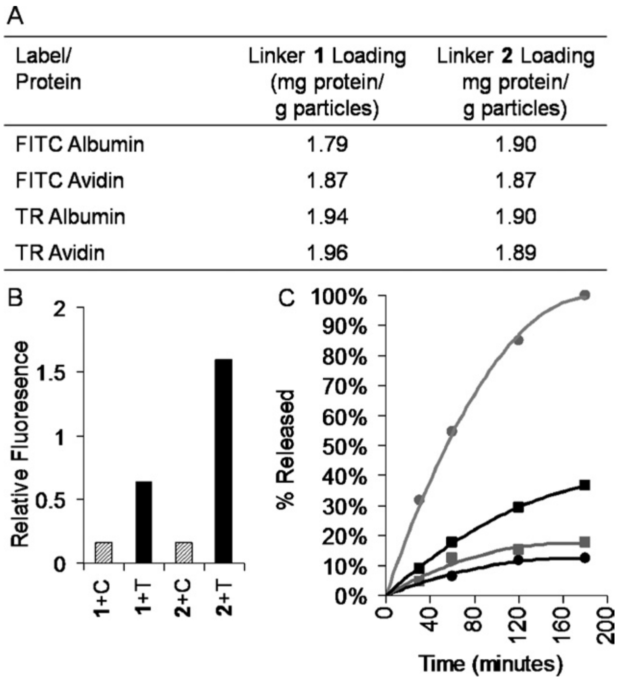

Label/ Protein	Linker **1** Loading (mg protein/ g particles)	Linker **2** Loading mg protein/ g particles)
FITC Albumin	1.79	1.90
FITC Avidin	1.87	1.87
TR Albumin	1.94	1.90
TR Avidin	1.96	1.89

Fig. 2 A) The loading values of the different label/proteins tested into **1** and **2**. B) Release of Texas Red-labelled albumin from **1** and **2** upon incubation with chymotrypsin (C) or thermolysin (T) for 3 hours. C) Comparative fluorescence release profiles of FITC-labelled **1**-albumin (▨), **2**-albumin (⊗), **1**-avidin (■), **2**-avidin (●).

molecules that complements the release of positively-charged avidin.

In conventional enzyme-triggered drug-release systems that rely on payload molecules that are covalently linked to a polymeric material *via* cleavable linkers, the enzymatic hydrolysis rate directly dictates drug release (*i.e.* one enzyme hydrolysis event releases one drug molecule). An exception is the system developed by Shabat *et al.*, that demonstrates the use of self-immolative dendron with multiple drug molecules, which are released by a single triggering event.[10] In the system described here, the protein loading is independent from the number of peptide actuators incorporated and release rates are therefore less dependant on enzyme kinetics. To test the sensitivity to enzyme concentration, it was varied over 4 orders of magnitude. As is clear from Fig. 3, in each case the release rates varied by less than one order of magnitude over the first 2 hours, clearly demonstrating that the release kinetics of the system described here is less reliant on enzyme levels.

Two-photon microscopy (TPM) was used to monitor spatio-temporal changes within the particles during release experiments. This method was previously found to be useful to assess enzymatic diffusion rates in PEGA beads.[11,12] Naturally, a release mechanism based on electrostatic interactions will depend on ionic strength, as will be discussed later. For the purpose of studying the molecular events during the initial stages of triggered release by TPM, buffer concentrations were kept at a minimum level to enhance the electrostatic interactions that are thought to underlie the release mechanism. Therefere, lyophilised enzyme powders were supplied in purified water, relying on associated buffer salts for pH control. TPM was used to monitor molecular activity within the particles during the initial stages of release of labelled protein molecules. This 45 minute time was chosen as it represents the time it takes for thermolysin to diffuse to the core of PEGA particles.[11] TR labelling (a pH-independent fluorophore) allows protein migration to be followed, whilst FITC (a pH-sensitive label) in addition gives insight into localised pH changes. Hence, fluorescence changes related to protein migration and local enzyme activity could be studied separately.

First, the release profile of TR-labelled albumin was studied from **1** and **2**. Equatorial cross-sectional images were taken every minute during 45 minutes. Image analysis was then performed to provide a detailed description of albumin release from **1** and **2**. The averaged pixel intensity of cross-sectional images indicates the amount of labelled protein present within a single particle allowing the amount and rate of release to be determined. As previously observed (Fig. 2C) there was some release of albumin from **1**, and the rate of release slowed after approximately 25 minutes (Fig. 4A). Approximately 30% of the payload, TR–albumin, was released from the hydrogel particle over 45 minutes. TR–albumin release from **2** proceeded in a distinctly different manner. A fluorescent band (TR–albumin) initially diffused towards the core of the particle, away from the negative charge that resulted from enzymatic hydrolysis on the particle's exterior. This is a three-dimensional process that appears as a spike in fluorescence in the two-dimensional cross-section (Fig. 3A). After approximately 20 minutes the expulsion of TR–albumin from the particle core was observed, suggesting that enzymes have reached the core of the particle, that is now negatively charged throughout. This point is signified by a precipitous decrease in the pixel intensity as the albumin molecules are expelled through the particle pores. As a result, a 50% decrease in pixel intensity over the first 45 minutes of exposure of **2**/TR–albumin particles to thermolysin, provides further evidence of the ability to control payload release through the design of the peptide.

TR-labelled avidin was used to complete the picture of release events (Fig. 5). During the thermolysin-induced release of TR–

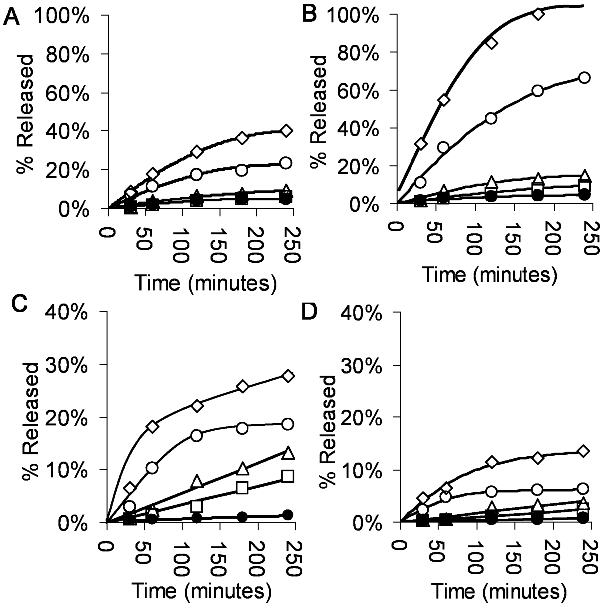

Fig. 3 Fluorescent release profiles of FITC-labelled albumin from A) **1** and B) **2**; FITC–avidin from C) **1** and D) **2** using 2 mg mL^{-1} (◇), 0.2 mg mL^{-1} (○), 0.02 mg mL^{-1} (Δ), and 0.002 mg mL^{-1} (□) thermolysin and chymotrypsin (●).

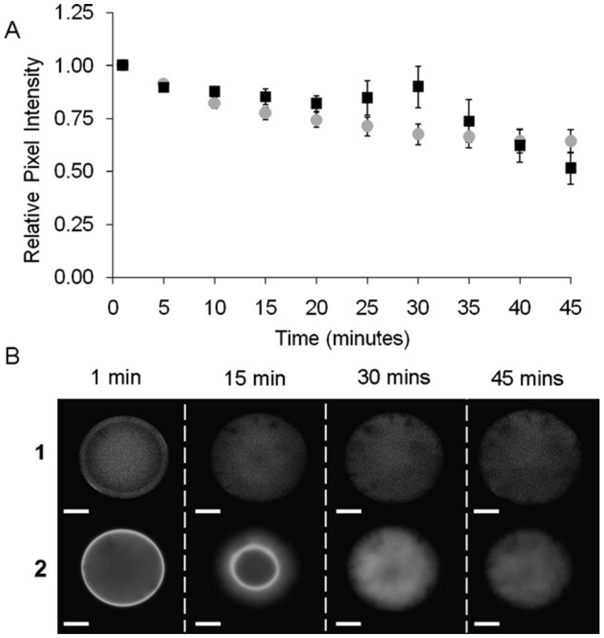

Fig. 4 A) Pixel intensity plots corresponding to TR conjugated albumin release from **1** (⊗) and **2** (■). B) TPM micrographs showing the release of TR-labelled albumin from **1** and **2**. Scale bar represents 75 μm.

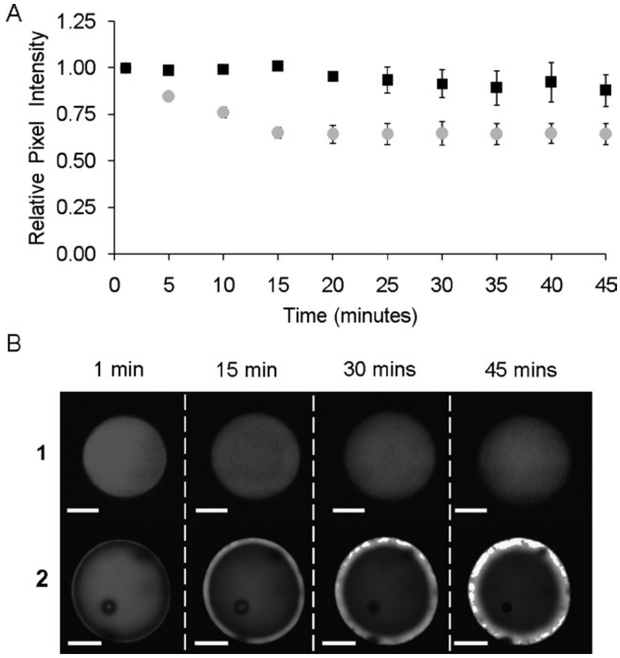

Fig. 5 A) Pixel intensity plots corresponding to TR-conjugated avidin release from **1** (⊗) and **2** (■). B) TPM micrographs showing the release of TR-labelled avidin from **1** and **2**. Scale bar represents 100 μm.

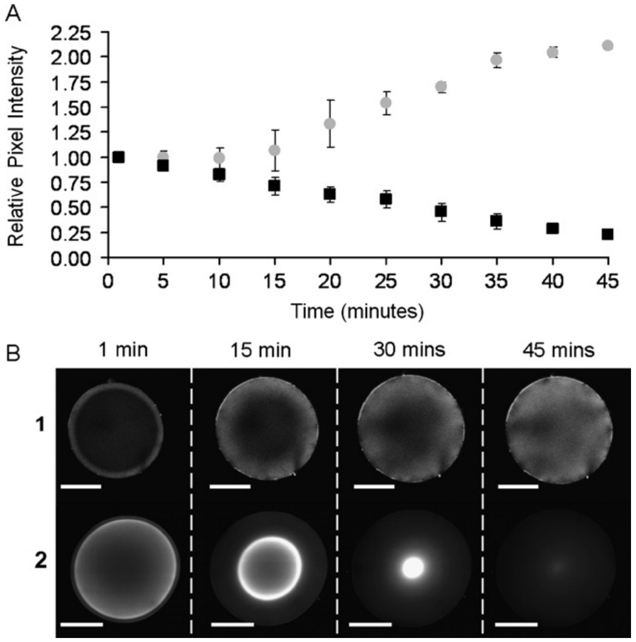

Fig. 6 A) Pixel intensity plots corresponding to FITC-conjugated albumin release from **1** (⊗) and **2** (■). B) TPM micrographs showing the release of FITC-labelled albumin from **1** and **2**. Scale bar represents 100 μm.

avidin from **1**, a 40% decrease in pixel intensity was observed within 15 minutes, corresponding to the exclusion of avidin from the particle core. In contrast, little release of TR–avidin was observed from **1**, due to the attractive interactions between TR–avidin and the particle following the hydrolysis reaction. Interestingly, a significant amount of TR–avidin appeared to concentrate at the periphery of the particle, which may show that enzyme activity occurs most extensively at the periphery of the particle. Gratifyingly, the trends observed in release profiles obtained from bulk fluorescence and microscopy agree in each case.

The pH responsiveness of FITC[13] provides an opportunity to follow localised pH changes within hydrogel particles during release experiments. After hydrolysis of **1** and rapid diffusion of mobile fragments, polymer-bound Ala–Arg results in an expected increase in localised pH, while the polymer-bound fragments Ala–Asp–Asp for **2** would result in a drop in localised pH. Enzyme action during the release of FITC-labelled albumin from **1** is shown in Fig 6. Pixel intensity plots reveal the expected highly contrasting fluorescence intensity changes that depend on the peptide selected. The increase in net fluorescence intensity during thermolysin cleavage of **1**/FITC–albumin suggests that the FITC–albumin is held within the particles and that there is an increase in local pH, as FITC fluorescence increases with increasing pH. The reverse effect is observed for thermolysin cleavage of **2**/FITC–albumin, which when coupled to the egress of FITC–albumin from the bead gives a strong decrease in fluorescence intensity. In both cases, the corresponding TPM micrographs suggest that peptide hydrolysis proceeds from the exterior of the particles inwards, but opposing charges remaining for the particles result in contrasting fluorescence cross-sections. For the **1**/FITC–albumin particles, the increase in local pH progresses inwards, but FITC–albumin is not released. For the **2**/FITC–albumin particles, FITC–albumin is simultaneously electrostatically driven out of the beads and concentrated in the centre, to give a central bright area surrounded by a FITC–albumin free shell.

Similarly, TPM was used to monitor the release of FITC-labelled avidin from **1** and **2** (Fig. 7). As before, the pixel intensity plots were dramatically different after hydrolysis of **1** and **2** by thermolysin. For the **1**/FITC–avidin beads, the increase in FITC fluorescence due to the increase in local pH after peptide hydrolysis is matched by the loss of FITC–avidin, to give little net change in fluorescence. This is shown in the TPM micrographs, which show a ring of fluorescence progressing from the exterior inwards, as the cleaved fragments diffuse out of the particle and the local pH is raised by the positively charged Ala–Arg-containing polymer chains. However, the converse occurs in the **2**/FITC–avidin particles, with thermolysin action causing a decrease in local pH and decreasing fluorescence, but with no corresponding release of FITC–avidin. The FITC–avidin is electrostatically held within the hydrogel matrix, but thermolysin action now causes a dark ring (indicating lowered pH) to progress from the bead exterior inwards.

Enzyme diffusion rates can be estimated from these data – it takes approximately 45 minutes for protease activity to be observed in the core of the particles. This is in agreement with previous reports,[11,12] indicating that electrostatic interactions between proteases and particles have little effect on diffusion rates.

Naturally, exploiting protease activity to affect protein release may result in undesired proteolysis of the payload protein, especially at high protease concentrations. MALDI-TOF mass spectroscopy analysis of the protein released from particles after

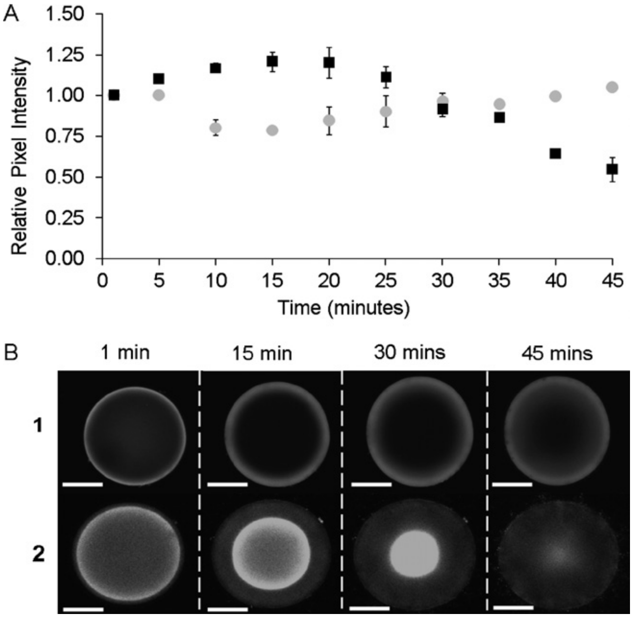

Fig. 7 A) Pixel intensity plots corresponding to FITC conjugated avidin release from **1** (⊗) and **2** (■). B) TPM micrographs showing the release of FITC-labelled avidin from **1** and **2**. Scale bar represents 100 μm.

4 hours incubation with thermolysin (at the highest concentration used, 2 mg mL^{-1}) gave rise to peaks assigned to the payload proteins or thermolysin (Fig. S1, ESI†). Hence, although proteolysis is probably unavoidable, it is not a major concern with the payload–protease combinations studied here.

As actuation of these particles is governed by electrostatic interactions, triggered release is sensitive to ionic strength due to electrostatic screening effects. To study this effect, FITC–albumin release was studied at 150, 15, 1.5 and 0.15 mM K^+/phosphate buffer at pH 7.4. Enzyme-triggered release was observed in each case, but the presence of 15 mM phosphate buffer reduced the released amount over 45 minutes by approximately 50% (Fig. S2, ESI†) whilst at physiological concentrations (150 mM) the release rate was insignificant. We are currently developing new peptide actuators to address this issue.

4. Conclusions

In summary, we have devised a drug-release mechanism, where guest molecules are only released upon the action of a specific protease. The release can be controlled by matching the charge on the peptide actuator to the charge on the payload protein. The combined use of a pH-sensitive label (FITC) with a pH-insensitive label (TR) allowed the molecular events related to enzyme action and protein release within the particles to be studied separately. This approach provided insight into the release profiles of these enzyme-triggered hydrogel particles. An important remaining challenge is to adapt these systems to high ionic strength (physiological) environments.

5. Acknowledgements

The authors wish to thank Versamatrix A/S for the generous gift of PEGA particles, Robert Fernandez for his technical assistance with two-photon microscopy, and Neil Bell for help with MALDI-TOF mass spectroscopy. The authors also thank Prof. Andrew Lyon (Georgia Institute of Technology, USA) for use of and assistance with transmission optical microscopy experiments.

6 References

1 (*a*) R. V. Ulijn, *J. Mater. Chem.*, 2006, **16**, 2217–2225; (*b*) D. G. Anderson, J. A. Burdick and R. Langer, *Science*, 2004, **305**, 1923–1924; (*c*) C. Alexander and K. M. Shakesheff, *Adv. Mater.*, 2006, **18**, 3321–3328; (*d*) Z. M. Yang, G. L. Liang and B. Xu, *Soft Matter*, 2007, **2**, 515–520; (*e*) A. S. Hoffman in *Biomaterials Science: An Introduction to Materials in Medicine*, ed. B. D. Ratner, A. S. Hoffman, F. J. Schoen, J. E. Lemons, Elsevier, 2nd edn, 2004, ch. 2, p. 107.

2 (*a*) R. Duncan, *Nat. Rev. Drug Discovery*, 2003, **2**, 347–360; (*b*) M.-R. Lee, K.-H. Baek, H. J. Jin, Y.-G. Jung and I. Shin, *Angew. Chem., Int. Ed.*, 2004, **43**, 1675–1678; (*c*) C. Li, J. Madsen, S. P. Armes and A. L. Lewis, *Angew. Chem., Int. Ed.*, 2006, **45**, 3510–3513; (*d*) K. N. Plunkett, K. L. Berkowski and J. S. Moore, *Biomacromoles*, 2005, **6**, 632–637; (*e*) B. Law, R. Weissleder and C.-H. Tung, *Biomacromoles*, 2006, **7**, 1261–1265; (*f*) K. J. C. Van Bommel, M. C. A Stuart, B. L. Feringa and J. Van Esch, *Org. Biomol. Chem.*, 2005, **3**, 2917–2920; (*g*) D. G. Vartak and R. A. Gemeinhart, *J. Drug Targeting.*, 2007, **15**, 1–21; (*h*) R. J. Amir, M. Popkov, R. A. Lerner, C. F. Barbas III and D. Shabat, *Angew. Chem., Int. Ed.*, 2005, **44**, 4378–4381; (*i*) F. M. H. de Groot, E. W. P. Damen and H. W. Scheeren, *Curr. Med. Chem.*, 2001, **8**, 1093–1122.

3 (*a*) J. F. Tolborg, L. Petersen, K. J. Jensen, C. Mayer, D. L. Jakeman, R. A. J. Warren and S. G. Withers, *J. Org. Chem.*, 2002, **67**, 4143–4149; (*b*) R. V. Ulijn, B. Baragana, P. J. Halling and S. L. Flitsch, *J. Am. Chem. Soc.*, 2002, **124**, 10988–10989; (*c*) R. M. Kohli, M. D. Burke, J. Tao and C. T. Walsh, *J. Am. Chem. Soc.*, 2003, **125**, 7160–7161; (*d*) M. Meldal, *Biopolymers*, 2002, **66**, 93–100; (*e*) M. Meldal, *Curr. Opin. Chem. Biol.*, 2004, **8**, 238–244; (*f*) J. Kress, R. Zanaletti, A. Amour, M. Ladlow, J. G. Frey and M. Bradley, *Chem.–Eur. J.*, 2002, **8**, 3769–3772.

4 "A co-polymer of polyethylene glycol and acrylamide, 800 denoting the molecular weight of the PEG chains", M. Meldal, Tetrahedron Lett., , 1992, , **33**, 3077–3080.

5 (*a*) P. D. Thornton, R. J. Mart and R. V. Ulijn, *Adv. Mater.*, 2007, **19**, 1252–1256; (*b*) P. D. Thornton, G. McConnell and R. V. Ulijn, *Chem. Commun.*, 2005, **47**, 5913–5915.

6 R. Haag and F. Kratz, *Angew. Chem., Int. Ed.*, 2006, **45**, 1198–1215(*a*) F. Kratz and U. Beyer, *Drug Delivery*, 1998, **5**, 281–299.

7 B. Schmid, D.-E. Chung, A. Warnecke, I. Fichtner and F. Kratz, *Bioconj. Chem.*, 2007, **18**, 702–716.

8 S. J. Todd, D. Farrar, J. E. Gough and R. V. Ulijn, *Soft Matter*, 2007, **3**, 547–550.

9 (*a*) K. Morihara, H. Tsuzuki and T. Oka, *Arch. Biochem. Biophys.*, 1968, **123**, 572; (*b*) *Enzymes of Molecular Biology*, ed. M. M. Burrell, Humana, Totowa, NJ 1993, vol. 16pp. 277–281; (*c*) K. A. Walsh, *Epistem. Epeteris Sch. Phys. Math. Epistem.*, 1970, **19**, 41.

10 A. Sagi, E. Segal, R. Satchi-Fainaro and D. Shabat, *Bioorg. Med. Chem.*, 2007, **15**, 3720–3727.

11 A. Y. Bosma, R. V. Ulijn, G. McConnell, J. Girkin, P. J. Halling and S. L. Flitsch, *Chem. Commun.*, 2003, 2790–2791.

12 J. Deere, G. McConnell, A. Lalaouni, B. A. Maltman, S. L. Flitsch and P. J. Halling, *Adv. Synth. Catal.*, 2007, **349**, 1321–1326.

13 *Molecular Fluorescence: Principles and Applications*, ed. B. Valeur, Wiley-VCH, Weinheim, 2001, ch. 10, p 285.